JOURNAL OF VIROLOGY, Sept. 2010, p. 8446–8459 Vol. 84, No. 17
0022-538X/10/$12.00 doi:10.1128/JVI.01416-09

Coxsackievirus B3 Infection Activates the Unfolded Protein Response and Induces Apoptosis through Downregulation of p58^{IPK} and Activation of CHOP and SREBP1$^{\nabla}$

Huifang M. Zhang,[1] Xin Ye,[1] Yue Su,[1] Ji Yuan,[1] Zhen Liu,[1] David A. Stein,[2] and Decheng Yang[1]*

Department of Pathology and Laboratory Medicine, University of British Columbia, The Providence Heart and Lung Institute, St. Paul's Hospital, Vancouver, British Columbia, Canada,[1] and Vaccine and Gene Therapy Institute, Oregon Health and Science University, Beaverton, Oregon 97006[2]

Received 9 July 2009/Accepted 7 June 2010

Cardiomyocyte apoptosis is a hallmark of coxsackievirus B3 (CVB3)-induced myocarditis. We used cardiomyocytes and HeLa cells to explore the cellular response to CVB3 infection, with a focus on pathways leading to apoptosis. CVB3 infection triggered endoplasmic reticulum (ER) stress and differentially regulated the three arms of the unfolded protein response (UPR) initiated by the proximal ER stress sensors ATF6a (activating transcription factor 6a), IRE1-XBP1 (X box binding protein 1), and PERK (PKR-like ER protein kinase). Upon CVB3 infection, glucose-regulated protein 78 expression was upregulated, and in turn ATF6a and XBP1 were activated via protein cleavage and mRNA splicing, respectively. UPR activity was further confirmed by the enhanced expression of UPR target genes ERdj4 and EDEM1. Surprisingly, another UPR-associated gene, p58^{IPK}, which often is upregulated during infections with other types of viruses, was downregulated at both mRNA and protein levels after CVB3 infection. These findings were observed similarly for uninfected Tet-On HeLa cells induced to overexpress ATF6a or XBP1. In exploring potential connections between the three UPR pathways, we found that the ATF6a-induced downregulation of p58^{IPK} was associated with the activation of PKR (PERK) and the phosphorylation of eIF2α, suggesting that p58^{IPK}, a negative regulator of PERK and PKR, mediates cross-talk between the ATF6a/IRE1-XBP1 and PERK arms. Finally, we found that CVB3 infection eventually produced the induction of the proapoptoic transcription factor CHOP and the activation of SREBP1 and caspase-12. Taken together, these data suggest that CVB3 infection activates UPR pathways and induces ER stress-mediated apoptosis through the suppression of P58^{IPK} and induction/activation of CHOP, SREBP1, and caspase-12.

Coxsackievirus B3 (CVB3) is a single-stranded positive-sense RNA virus of the genus *Enterovirus* in the family *Picornaviridae* and can cause acute or chronic viral myocarditis. Epidemiological studies reveal that viral myocarditis is one of the major heart diseases worldwide, particularly in infants, children, and adolescents (17). Further, CVB3-induced myocarditis can result in dilated cardiomyopathy, a condition for which the only treatment is heart transplantation (12). CVB3 infection has been studied for decades in various systems, but the mechanisms of pathogenesis underlying CVB3-induced myocarditis in humans remain poorly defined. Cumulative evidence suggests that both direct viral injury and subsequent inflammatory responses contribute to the damage of cardiac myocytes, and that the extent of such damage determines the severity of late-stage heart dysfunction (10, 35). Previous studies have documented that apoptosis in cardiomyocytes can result in damaged myocardial tissue and is a hallmark of CVB3-induced myocarditis (1, 45). Although it has been shown that apoptosis facilitates the release of viral progeny during CVB3 infection (9, 48), the molecular events leading to apoptosis in CVB3-infected cells have not been well characterized.

The endoplasmic reticulum (ER) system, a primary site for protein synthesis and folding, is a major site of signal initiation and transduction in response to a variety of stimuli, including virus infections (24, 66). Endogenous imbalances in cells, such as the overproduction of proteins, the accumulation of mutant proteins, or the loss of calcium homeostasis, can cause a malfunction of cellular processes and stress to the ER system (26). In response to ER stress, a coordinated adaptive program called the unfolded protein response (UPR) is activated and serves to minimize the accumulation and aggregation of misfolded proteins by increasing the capacity of the ER machinery to fold proteins correctly and activate the degradation of aberrant proteins. The UPR program represents a network of signal transduction from the ER to various locations within the cytoplasm and the nucleus, resulting in either the enhancement of cell survival or the induction of apoptosis (5). Glucose-regulated protein 78 (GRP78) functions as a master regulator of the UPR, and its upregulation indicates the activation of the UPR program (18, 27, 44). Under normal conditions, GRP78 is associated with stress sensor proteins in the ER luminal domain. Under stress conditions, GRP78 is released and binds to misfolded proteins, resulting in the activation of stress sensors (22).

The UPR network of interactions is considered to have

* Corresponding author. Mailing address: The iCapture Center, Heart and Lung Institute, University of British Columbia, St. Paul's Hospital, 1081 Burrard St., Vancouver, British Columbia, Canada V6Z 1Y6. Phone: (604) 682-2344, ext. 62872. Fax: (604) 806-9274. E-mail: decheng.yang@hli.ubc.ca.

$^{\nabla}$ Published ahead of print on 16 June 2010.

three major arms, each activated by a characteristic sensor, PERK (PKR-like ER protein kinase), IRE1 (inositol-requiring enzyme 1), and ATF6a (activating transcription factor 6a) (59). The activation of the PERK pathway results in the phosphorylation of the eukaryotic translation initiation factor 2α (eIF2α) subunit, leading to translation attenuation (18). PERK also activates the expression of ATF4, a transcription factor, leading to an upregulation of the proapoptotic genes CHOP (c/EBP homologous protein) and GADD34 (growth arrest and DNA damage-inducible protein-34) (38). IRE1 is a bifunctional ER transmembrane protein with both serine-threonine kinase and RNase activities (52, 56). Upon activation, IRE1 can remove a 26-nucleotide (nt) intron from unspliced X box binding protein 1 (XBP1) mRNA (XBP1u) by RNase activity, resulting in a translational frameshift. The spliced form of XBP1 mRNA (XBP1s) encodes a protein with a novel C terminus and acts as a potent transcriptional activator of many genes involved in the UPR (42). ATF6a is an ER transmembrane protein residing in the cytosol under normal physiological conditions. Upon the accumulation of misfolded proteins in the ER, ATF6a migrates to the Golgi apparatus, where it is cleaved by S1P and S2P proteases, releasing a soluble fragment that enters the nucleus and activates the transcription of ER chaperones and other genes responsible for correct protein folding (20).

A number of viruses have been shown to trigger ER stress upon infection. However, the pattern of molecular interactions that occurs within the UPR program differs depending on virus identity and type of host cell. Many viruses apparently activate only one or a subset of UPR pathways, and interestingly, some viral infections activate one pathway yet suppress others. For example, the expression of hepatitis C virus (HCV) proteins activates the PERK- and ATF6a-initiated pathways (4, 8, 40) yet suppresses the IRE1-XBP1 pathway (51). Similarly, human cytomegalovirus (CMV) activates PERK and IRE1-XBP1 but suppresses the ATF6a pathway (23, 53).

In this study, with the use of mouse cardiomyocytes and unmodified HeLa cells, as well as HeLa cell lines engineered to inducibly express genes integral to the UPR, we focus on the mechanisms of linkage between the ER stress response to CVB3 infection and the induction of apoptosis. We found that CVB3 infection activates ER stress effectors and differentially regulates the three arms of the UPR. CVB3 infection produced a downregulation of $p58^{IPK}$ and associated enhancement of PKR (PERK) phosphorylation activity, and these alterations affected the other two arms of the UPR. Subsequently, the proapoptotic proteins CHOP, SREBP1 (sterol regulatory element binding protein 1), and caspase-12 can become induced. Taken together, these activities appear to participate in a coordinated shifting of the ER stress response to an apoptotic program in CVB3-infected cells.

MATERIALS AND METHODS

Virus, cells, siRNAs, plasmids, and transfections. CVB3 (CG strain) was obtained from Charles Gauntt (University of Texas Health Science Center) and propagated in HeLa cells (ATCC). Virus stock was isolated from cells by three freeze-thaw cycles followed by centrifugation to remove cell debris and was stored at −80°C. The titer of virus stock was determined by plaque assay as described previously (67) and below. HeLa cells were grown in Dulbecco's modified Eagle's medium (DMEM) supplemented with 100 μg/ml penicillin, 100 μg/ml streptomycin, 2 mM glutamine, and 10% fetal bovine serum (FBS) (Clontech). The HL-1 cell line, a mouse cardiac muscle cell line established from a cardiomyocyte tumor lineage, was a gift from William C. Claycomb (Louisiana State University Health Science Center). HL-1 cells were maintained in Claycomb medium (11) supplemented with 10% FBS (JRH Biosciences), 100 μg of penicillin-streptomycin/ml, 0.1 mM norepinephrine (Sigma), and 2 mM L-glutamine (Invitrogen). The individual short interfering RNAs (siRNAs) targeting human or mouse XBP1 and human ATF6a and GRP78 were purchased from Santa Cruz Biotech and transfected according to the manufacturer's instructions. Briefly, 2×10^5 HeLa cells were grown at 37°C overnight to 60 to 70% confluence in 6-well plates, washed with phosphate-buffered saline (PBS), and overlaid for 24 h with transfection complex containing siRNA and Oligofectamine (Invitrogen). The transfection medium then was replaced with DMEM containing 10% FBS, and the incubation was continued for 48 h. The transfection of plasmid pcDNA1/neo-$p58^{IPK}$ (a gift from Michael Katze, University of Washington) and pcDNA3.1-ATF6(171-373) (a gift from K. Mori, Kyoto University, Kyoto, Japan) into HeLa cells was conducted by the same procedures as those for siRNA described above, except Lipofectamine (Invitrogen) was the transfection reagent.

Construction of pTRE-HA-XBP1u-GFP and pTRE-HA-ATF6a and production of double-stable Tet-On/HeLa cell lines. cDNA of XBP1u fused with GFP (green fluorescence protein) was amplified from the plasmid pHA-XBP1u-GFP (a gift from Yi-Ling Lin, Academia Sinica, Taiwan, Republic of China) by PCR using primers listed in Table 1. The fragments were digested by HindIII and XbaI and ligated into the pTRE-HA vector (Clontech). The recombinant plasmid was confirmed by DNA sequencing. The full-length cDNA of ATF6a was amplified by PCR from the plasmid pCMV-ATF6a (OriGene, Rockville, MD) using primers listed in Table 1. The pTRE-HA-ATF6a expression plasmid was constructed by using the same strategy as that for constructing pTRE-HA-XBP1u-GFP.

The double-stable Tet-On cell line inducibly expressing ATF6a or XBP1 was established by plasmid transfection. Briefly, 10^5 Tet-On HeLa cells were cotransfected with either pTRE/HA-ATF6a or pTRE/HA-XBP1u-GFP, along with pTK-Hyg (encoding hygromycin resistance), using Lipofectamine (Invitrogen) according to the manufacturer's instructions. After 8 h of incubation with 4 μg of plasmid and Lipofectamine, the mixture was replaced with DMEM containing 10% FBS and hygromycin or G418 at a concentration of 200 or 400 μg/ml, respectively, and incubation was continued for 2 days before the initial selection of double-stable cells. Doubly resistant clones were picked 3 weeks later and further screened for ATF6a or XBP1 protein expression by Western blotting using the hemagglutinin (HA) antibody (Covance). Cells transfected with the empty vectors pTRE and pTK-Hyg also were selected by hygromycin and G418 in parallel for use as controls. To induce the expression of ATF6a or XBP1, cells were cultured for 12 to 72 h in medium containing 1 μg/ml doxycycline (Dox).

RNA preparation and RT-PCR analysis. Total RNA from cultured cells was isolated with the RNeasy Mini kit (Qiagen) by following the supplier's instructions. First-strand cDNAs were reverse transcribed (RT) with 3 μg of RNA as the template, and the target genes were amplified by PCR by following the procedures described in the one-step RT-PCR kit (Qiagen), with minor modifications. Briefly, 2 μg of first-strand cDNA and 100 ng of each primer (Table 1) were used for PCR under standard conditions for 30 cycles, a point confirmed as falling within the exponential phase of amplification.

Western blot analysis. Western immunoblotting was performed by standard protocols as previously described (32). Briefly, cells were washed with cold PBS before the addition of an appropriate volume of lysis buffer (0.025 M Tris-HCl, pH 8.0, 137 mM NaCl, 10% glycerol, 1 mM EDTA, 1 mM EGTA, 1% Triton X-100, and proteinase inhibitor cocktail). After incubation for 20 min on ice, the cell lysates were centrifuged at 13,000 × *g* for 15 min at 4°C, and protein-containing supernatant was collected. For protein isolation, the NE-PER nuclear and cytoplasmic extraction reagents (Pierce) were employed per the manufacturer's instructions. The isolated proteins were separated by 10% SDS-PAGE and transferred onto nitrocellulose membranes. Membranes were blocked with 5% skim milk in PBS and incubated with one of the following primary antibodies: monoclonal anti-human GRP78 (Transduction Laboratory), monoclonal anti-mouse actin (Sigma), monoclonal mouse anti-HA.11 (Covance), monoclonal mouse anti-VP1 (Novocastra), rabbit polyclonal anti-human caspase-7, polyclonal anti-human p-eIF2α, monoclonal anti-human $p58^{IPK}$ and polyclonal anti-mouse p-PERK (Cell Signaling), monoclonal anti-mouse caspase-12, polyclonal anti-human p-PKR, polyclonal anti-mouse ATF6a, polyclonal anti-mouse XBP1, polyclonal anti-human SREBP1, monoclonal anti-human caspase-3, monoclonal anti-human CHOP, and polyclonal anti-mouse histone H1 (Santa Cruz). After several washes with PBS, each blot was further incubated with an appropriate secondary

TABLE 1. Primer sequences used for RT-PCR to detect gene expression and for cloning to construct Tet-On plasmids

Target gene	Direction	Primer sequence (5′ to 3′)	Application
XBP1 (human)	Forward	CTGGAACAGCAAGTGGTAGA	
	Reverse	CTGGATCCTTCTGGGTAGAC	RT-PCR
XBP1 (mouse)	Forward	AAACAGAGTAGCAGCGCAGACTGC	
	Reverse	GGATCTCTAAAACTAGAGGCTTGGTG	RT-PCR
$p58^{IPK}$ (human)	Forward	GAGGTTTGTGTTGGGATGCAG	
	Reverse	GCTCTTCAGCTGACTCAATCAG	RT-PCR
$p58^{IPK}$ (mouse)	Forward	GAGGTTTGTGTTTGGGATGCAG	
	Reverse	TGAGCTGAAGGGATTGAACCC	RT-PCR
ERdj 4 (human)	Forward	AAAATAAGAGCCCGGATGCT	
	Reverse	CGCTTCTTGGATCCAGTGTT	RT-PCR
ERdj 4 (mouse)	Forward	TTAGAAATGGCTACTCCACAGTCA	
	Reverse	TTGTCCTGAACAATCAGTGTATGTAG	RT-PCR
EDEM (human)	Forward	TCATCCGAGTTCCAGAAAGCAGTC	
	Reverse	TTGACATAGAGTGGAGGGTCTCCT	RT-PCR
EDEM (mouse)	Forward	GCCTCCTTTCTGCTCACAGAATAATAA	
	Reverse	CTCCTTCTCCTTCATTGCAGGCT	RT-PCR
XBP1-GFP	Forward	GATCCACAAGCTTTAGTGGTG	
	Reverse	GCTCGAGCGTCTAGATTATTAGTACAG	Cloning
ATF6a	Forward	GGAGAAGAAGCTTGGGAAATGGGGGAG	
	Reverse	CAAAGCTTCTAGATGCTATTGTAATGACTC	Cloning

antibody (goat anti-mouse or donkey anti-rabbit) conjugated to horseradish peroxidase (Amersham). Detection was carried out by enhanced chemiluminescence (Amersham) and the manufacturer's instructions.

Cell viability assay. To determine the effect of ATF6a expression on cell viability, HeLa cells were left uninduced or were induced with Dox for 72 h and then infected with CVB3 at a multiplicity of infection (MOI) of 10 for 10 h. Cell viability was analyzed with a 3-(4-5-dimethylthiazol-2-yl)-5-(3-carboxymethoxyphenyl)-2-(4-sulfophenyl)-2H-tetrazolium salt (MTS) assay kit (Promega) by following the manufacturer's instructions. Briefly, cells were incubated with MTS solution for 4 h, after which the absorbance of formazon at 492 nm was measured using an enzyme-linked immunosorbent assay (ELISA) plate reader. The absorbance of sham-infected/not induced cells was defined as 100% survival (control), and the remaining data were converted to a percentage of the control.

Cell immunofluorescence assay. HeLa cells grown in 6-well plates to 80% confluence were transfected with plasmid pHA-XBP1u-GFP for 24 h and then infected with CVB3 at an MOI of 10 for 1 h by following methods described previously (68). After 8 h of incubation in fresh growth medium, the cells were washed with PBS and fixed with 2% paraformaldehyde. Cell morphology and GFP expression were observed and photographed under an inverted fluorescent microscope (Nikon).

Viral plaque assay. Viral titers were determined by plaque assay as described previously (67). Briefly, samples of cells and medium from plates receiving the various treatments were freeze-thawed and then centrifuged (4,000 × *g*) to isolate viruses. HeLa cells were seeded into 6-well plates (8×10^5 cells/well) and incubated at 37°C for 20 h to a confluence of approximately 90% and then washed with PBS and overlaid with 500 μl of virus-containing samples serially diluted in cell culture medium. After a viral adsorption period of 60 min at 37°C, the supernatant was removed and the cells overlaid with 2 ml of sterilized soft Bacto-agar-minimal essential medium, cultured at 37°C for 72 h, fixed with Carnoy's fixative for 30 min, and stained with 1% crystal violet. The plaques were counted and viral PFU per ml calculated.

Statistical analysis. The Student's *t* test was employed to analyze data. The results are expressed as means ± standard deviations (SD) of three independent experiments. A *P* value of less than 0.05 was considered statistically significant.

RESULTS

CVB3 infection induces ER stress, and silencing of GRP78 sensitizes cells to virus-induced death yet inhibits viral protein production. GRP78 upregulation is a major indicator of ER stress. To study the effect of CVB3 infection on ER homeostasis, we first determined the expression of GRP78 in both HeLa cells and HL-1 cardiomyocytes at various time points postinfection (pi). Figure 1A and B show that GRP78 expression gradually increased and reached a high level at 12 h pi in both cell lines, although the upregulation of GRP78 expression was more robust in HeLa cells than in HL-1 cells. The upregulation of GRP78 indicates that CVB3 infection induces ER stress.

As the activation of ER stress response pathways is a protective mechanism against aberrant protein production, we were interested to explore the effect of GRP78 silencing on CVB3 replication and CVB3-induced cell death. Figure 1C shows higher cell death in CVB3-infeceted cells transfected with GRP78 siRNA (image d) than in infected cells transfected with a negative control (scrambled sequence) siRNA (image b) or in sham-infected cells transfected with GRP78 siRNA (image c). This result indicates that reduced GRP78 expression sensitizes the cells to CVB3-induced cell death, and this was further confirmed by the decreased viability of cells treated with GRP78 siRNA compared to that of cells treated with scrambled siRNA (Fig. 1D). In CVB3-infected cells, the increased activation of caspase-3, along with reduced viral replication, as indicated by the relative levels of the major CVB3 structural protein VP1, were apparent in GRP78 siRNA-

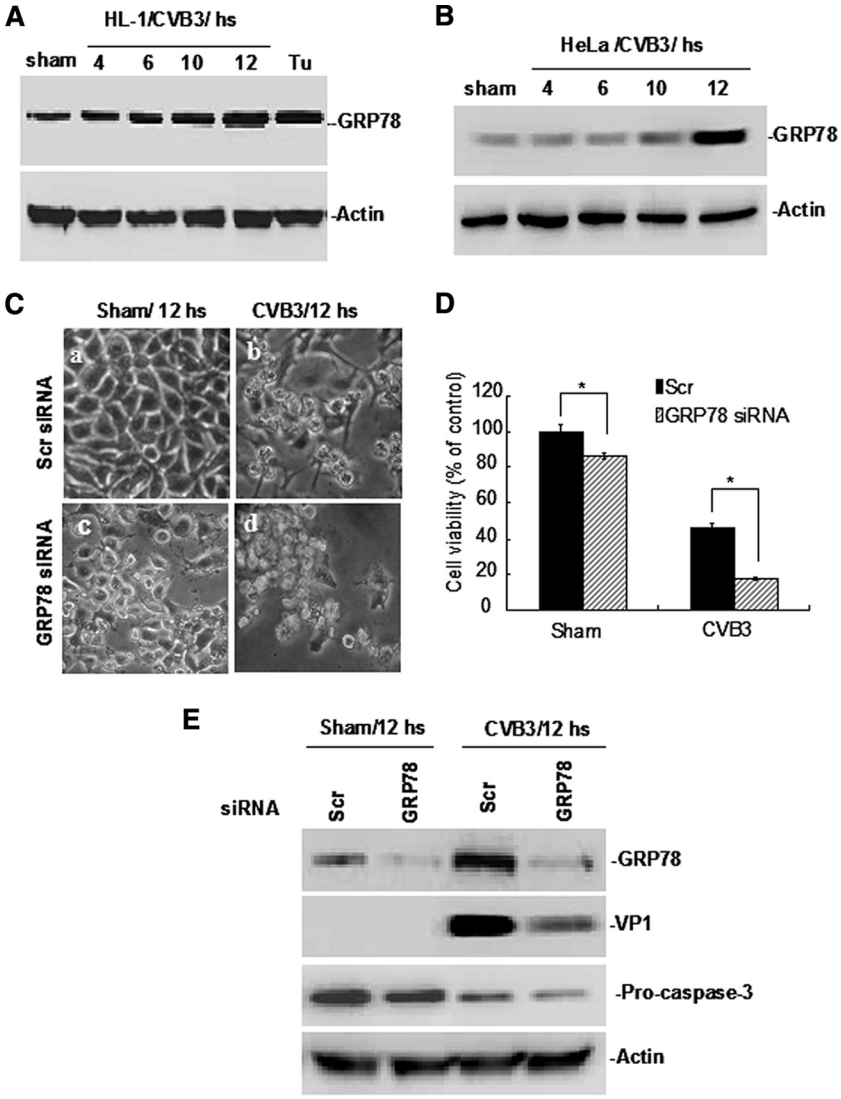

FIG. 1. CVB3 infection upregulates GRP78 expression, and the silencing of GRP78 enhances CVB3-induced cell death and reduces VP1 synthesis. Mouse cardiomyocyte HL-1 cells (A) and HeLa cells (B) were infected with CVB3 at an MOI of 100 and 10, respectively. The cell lysates were prepared at the indicated time points pi and subjected to Western blot analysis using the indicated antibodies. HeLa cells treated with tunicamycin (Tu) (2 mg/ml) to induce ER stress were included as a positive control. Actin is detected as a loading control. HeLa cells were transfected with GRP78 siRNA or scrambled (Scr) siRNA and then infected with CVB3. At 12 h pi, cell morphology was observed by phase-contrast microscopy (C), and cell viability was measured by MTS assay and converted to a percentage of a control receiving no siRNA transfection and sham infection (D). Error bars represent means ± SD. $P < 0.05$. (E) Relative levels of CVB3 VP1 protein and procaspase-3 cleavage were detected by Western blot analysis.

treated cells but not in those treated with scrambled siRNA (Fig. 1E).

CVB3 infection activates the XBP1 pathway but suppresses p58^{IPK} expression. It has been established that under ER stress conditions, IRE1 can become activated and direct the splicing of a 26-nucleotide (nt) intron from XBP1u, resulting in a translational frameshift of XBP1 mRNA (7). The gene product of XBP1s acts as a potent transcriptional activator of several genes involved in the UPR. To determine whether CVB3 infection can trigger XBP1 mRNA splicing, we employed the reporter plasmid pHA-XBP1u-GFP. This plasmid encodes an N-terminal HA-tagged XBP1u, with the C terminus fused to GFP at the second open reading frame (ORF) of XBP1u. The GFP is expressed only after XBP1u is spliced, thereby removing a 26-nt intron containing a PstI site (66). The confirmation of GFP expression was performed by fluorescence microscopy after the CVB3 infection of reporter plasmid-transfected cells. Figure 2A shows that GFP signal was apparent in both CVB3-infected HeLa cells and tunicamycin (Tu)-treated control cells transfected with reporter plasmids, but not in sham-infected or vector-transfected cells, indicating that XBP1 was correctly spliced. XBP1 splicing was further confirmed by RT-PCR detecting the XBP1u and XBP1s forms, as well as by the expression of downstream genes responsive to XBP1s. The data in Fig. 2B indicate the splicing of the PstI-containing intron, as the digestion of the PCR product with PstI did not produce the

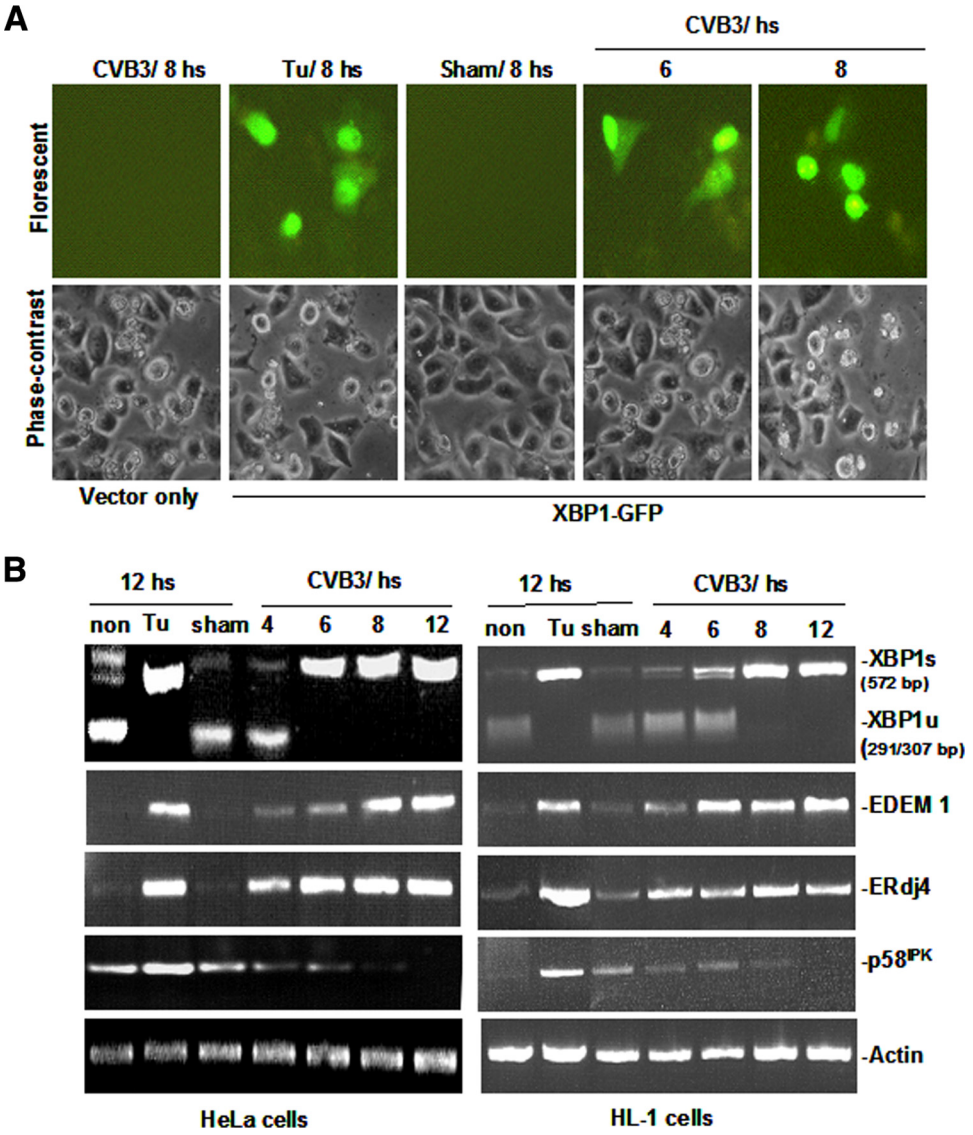

FIG. 2. CVB3 infection induces XBP1 mRNA splicing and alters the expression of its responsive genes. (A) Demonstration of XBP1 splicing by a GFP-based reporter in HeLa cells. Cells were transfected with pHA-XBP1u-GFP and then infected with CVB3, or sham infected with DMEM, or treated only with Tu at a final concentration of 2 mg/ml. Vector-transfected/CVB3-infected cells were included as an additional control. Reporter expression after XBP1 splicing was determined by fluorescent microscopy. (B) RT-PCR analysis. Both HeLa cells and HL-1 cells were infected with CVB3 or sham infected with DMEM. Total cellular RNAs were prepared at the indicated time points pi, and RT-PCRs were performed using specific primers to determine the level of XBP1 splicing and the expression of each indicated target gene. For detecting XBP1 splicing, PCR products were digested with PstI and electrophoresed. The XBP1u (291/307 bp) and XBP1 (572 bp) bands are indicated.

two fragments (291 and 307 nt) characteristic of unspliced RNA isolated from HeLa and HL-1 cells. The spliced XBP1s gene product further upregulated the expression of its target genes ERdj4 (ER-localized DnaJ4) and EDEM1 (ER degradation-enhancing α-mannosidase-like protein). To our surprise, $p58^{IPK}$, a cellular inhibitor of the eIF2α kinases PKR and PERK, which is often upregulated in association with the UPR, was downregulated in the setting of CVB3 infection.

Silencing XBP1 expression enhances CVB3-induced cell death and inhibits CVB3 VP1 synthesis. To further explore the function of XBP1 in the UPR, the effect of reduced XBP1 expression on cell survival and viral replication was investigated. The siRNA targeting of XBP1 significantly reduced the level of XBP1 mRNA and that of its downstream target genes EDEM1 and ERdj4 (Fig. 3A). In addition, HeLa cell death induced by CVB3 infection was greatly enhanced in XBP1 siRNA-transfected cells (Fig. 3B, image d) compared to that of controls (Fig. 3B, images b and c). The enhanced death of infected cells containing lowered levels of XBP1 mRNA was confirmed by cell viability assays (Fig. 3C), increased procaspase-3 cleavage (Fig. 3D), and decreased CVB3 VP1 protein synthesis (Fig. 3E).

Overexpression of XBP1 enhances UPR and promotes CVB3 VP1 protein synthesis. To further semiquantitatively determine the effect of XBP1 expression levels on cell survival and CVB3 replication efficiency, we established a Tet-On/

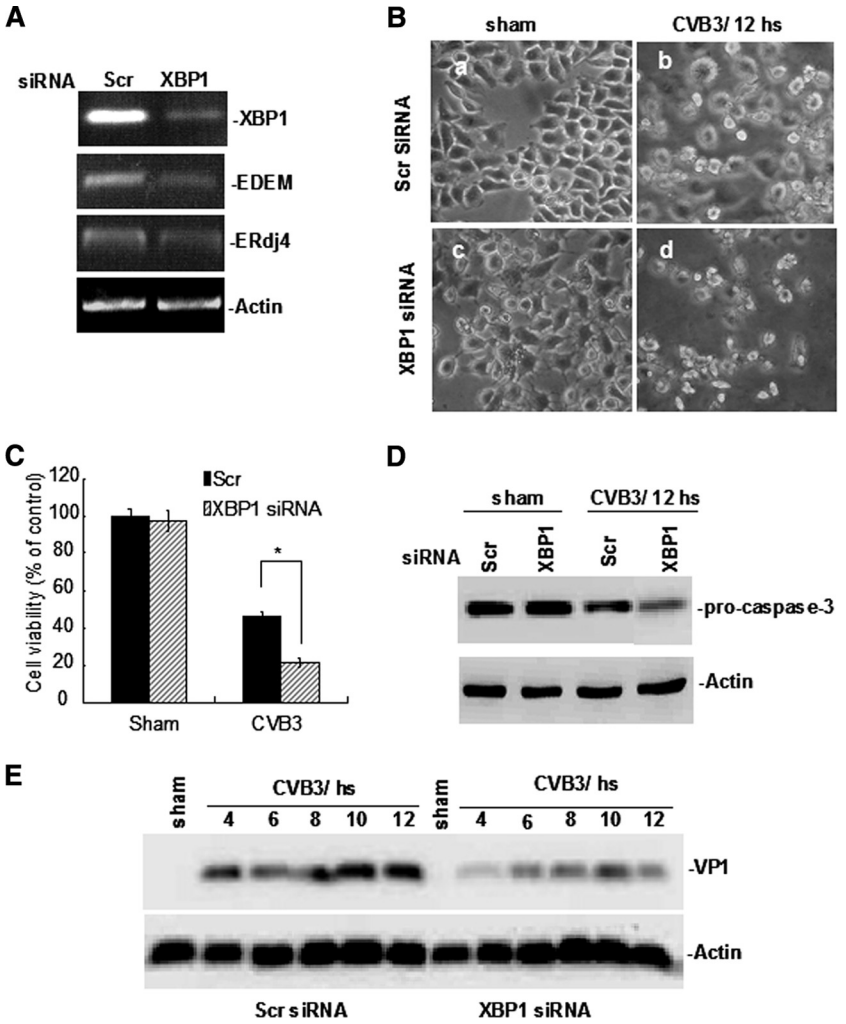

FIG. 3. Silencing of XBP1 enhances CVB3-induced cell death and reduces VP1 synthesis. (A) HeLa cells at 90% confluence were transfected with XBP1 siRNA or scrambled siRNA, and the expression of XBP1 as well as its responsive genes was determined by RT-PCR using primers listed in Table 1. siRNA-transfected HeLa cells were infected with CVB3 or sham infected with DMEM. (B) Cell morphology changes were observed by microscopy at 12 h pi. (C) Cell viability was measured by MTS assay and converted to a percentage of the control as described for Fig. 1. Error bars represent means ± SD. $P < 0.05$. In addition, procaspase-3 cleavage (D) and CVB3 VP1 production (E) were detected by Western blot analysis using the same amount of cell lysate for each time point. Actin was used as a loading control.

XBP1-inducible cell line to examine the effect of XBP1 expression on the upregulation of ER chaperone in the absence of CVB3 infection. Figure 4A shows that XBP1 expression was increased beginning at 12 h after Dox induction (pdi), and that this increase coincided with the upregulation of GRP78 and downregulation of $p58^{IPK}$. Further, the downregulation of $p58^{IPK}$ correlated with the increased phosphorylation of PKR and eIF2α (Fig. 4A). Second, we examined the effect of XBP1 expression on CVB3 replication at different time points after infection. Tet-On/XBP1 HeLa cells were induced for 72 h with Dox to promote XBP1 expression and then infected with CVB3. VP1 protein synthesis, viral plaque formation, and cell viability were evaluated at several time points pi. We found that the expression of GRP78 and CVB3 VP1 were significantly enhanced 6 h pi in Dox-induced cells compared to that in uninduced cells at the corresponding time points (Fig. 4B). However, CVB3 plaque formation data exhibited a converse pattern compared to that observed in the VP1 production data, with Dox-induced cells producing less infectious virus than uninduced cells (Fig. 4C). We speculate that this may be because XBP1 expression suppresses a later stage of the CVB3 life cycle, such as particle assembly, resulting in a decrease in infectious virus production. This speculation is further supported, at least in part, by cell viability data (Fig. 4D) showing that cells induced to express XBP1 and then infected with CVB3 have higher viability than uninduced and infected cells. Such higher viability may result from XBP1 expression suppressing CVB3 particle formation and thereby benefiting the health of host cells.

CVB3 infection activates the ATF6a pathway. In response to ER stress, ATF6a is cleaved in the Golgi apparatus by transmembrane proteases and translocated to the nucleus, where it activates genes responsible for UPR (20, 47). To assess whether CVB3 infection activates the ATF6a pathway, ATF6a cleavage was evaluated by the Western blot analysis of HeLa and HL-1 cell lysates prepared at various time points after

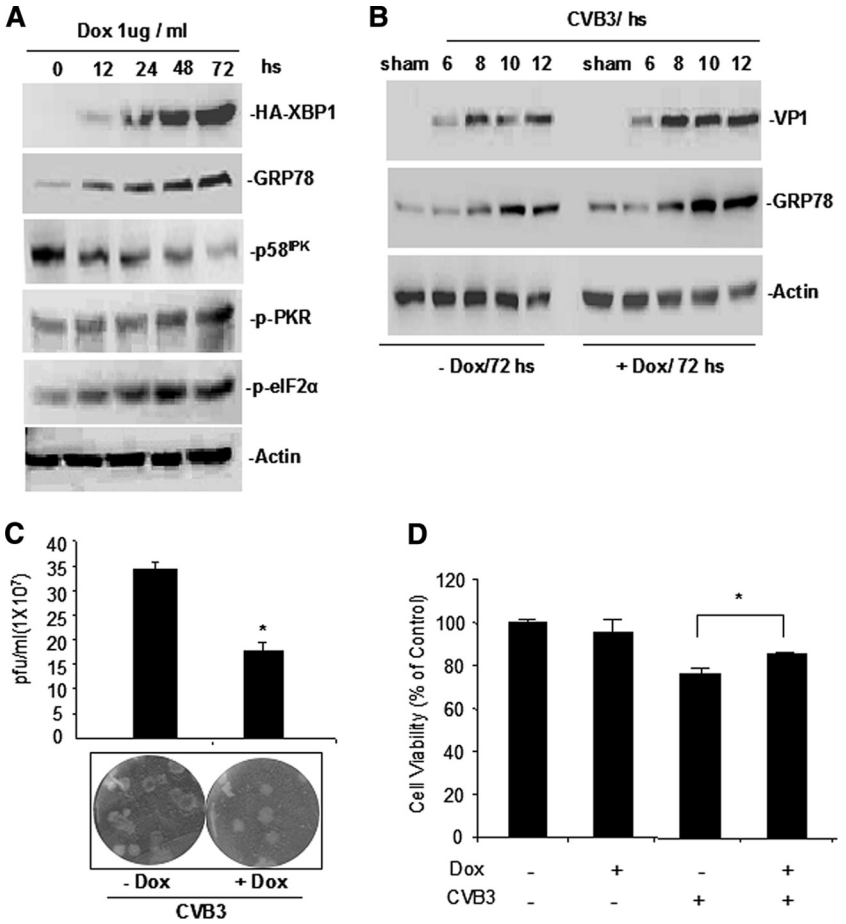

FIG. 4. Overexpression of XBP1 differentially alters target gene expression in the absence or presence of CVB3 infection. (A) Overexpression of XBP1 upregulates GRP78 but downregulates $p58^{IPK}$ in the absence of CVB3 infection. Tet-On/HA-XBP1 HeLa cells were induced (+Dox) or not induced (−Dox) for XBP1 expression. Cell lysates were subjected to Western blot analysis to detect XBP1 and its target genes, GRP78 and $p58^{IPK}$. (B) Overexpression of XBP1 promotes CVB3 VP1 protein synthesis. Tet-On/HA-XBP1 HeLa cells were left uninduced or were induced with Dox and then infected with CVB3. At the indicated time points pi, cell lysates were prepared for Western blot analyses of CVB3 VP1 and GRP78 proteins. Actin expression was detected in parallel as a loading control. (C) Viral plaque assay. CVB3 titer was determined at 12 h pi. An uninduced sample was included as a control. (D) Cell viability assay. An MTS assay was performed on the cells described above at 12 h pi. The data are presented as percentages of the uninduced/uninfected control. Error bars represent means ± SD. $P < 0.05$.

CVB3 infection. Figure 5A shows an intact form of ATF6a (90 kDa) detected in sham-infected cells, while in infected cells the cleavage of ATF6a, producing a 50-kDa band, was detectable at 8 h pi and almost complete at 12 h pi, indicating that CVB3 infection activates the ATF6a pathway in the two cell lines evaluated. To further evaluate the effect of ATF6a activation on cell viability and viral replication, we first used siRNAs targeting ATF6a and then measured the expression levels of ATF6a and its target gene XBP1 by Western blotting and RT-PCR, respectively. As shown in Fig. 5B, ATF6a expression was strongly reduced by its specific siRNA in uninfected cells. Cells that had been treated with ATF6a-siRNA were then infected with CVB3 and evaluated for viability, VP1 protein levels, infectious virus production, and changes in morphology. Figure 5C shows that, at each time point tested, VP1 protein synthesis was reduced in cells transfected with ATF6a siRNA compared to cells transfected with scrambled siRNA. Figure 5D shows that more cell death was observed in infected cells transfected with ATF6a siRNA (image d) than in controls (images b and c). This result was confirmed by the decreased cell viability (Fig. 5E) and increased cleavage of procaspase-3 (Fig. 5F) observed in ATF6a-siRNA treated cells compared to that in controls. We note that, as found in the experiments producing Fig. 1E and 3D, the cleavage product of procaspase-3 was difficult to detect by immunoblotting. It may be that the siRNA silencing of target genes contributed to CVB3-induced proteosome-mediated degradation of the procaspase form, precluding its detection (33, 50). To confirm the occurrence of cleavage, we performed additional Western blot analysis on 17% acrylamide resolving gels, loading 80 μg of total protein (instead of the usual 30 μg), and then were better able to detect the cleaved form (17 to 19 kDa) of caspase-3 (Fig. 5G).

Overexpression of ATF6a upregulates XBP1 and alters chaperone expression. To further determine whether transcription factor ATF6a regulates XBP1 and the expression of other downstream genes, we established a Tet-On/HA-ATF6a cell line that expresses ATF6a upon induction with Dox. To

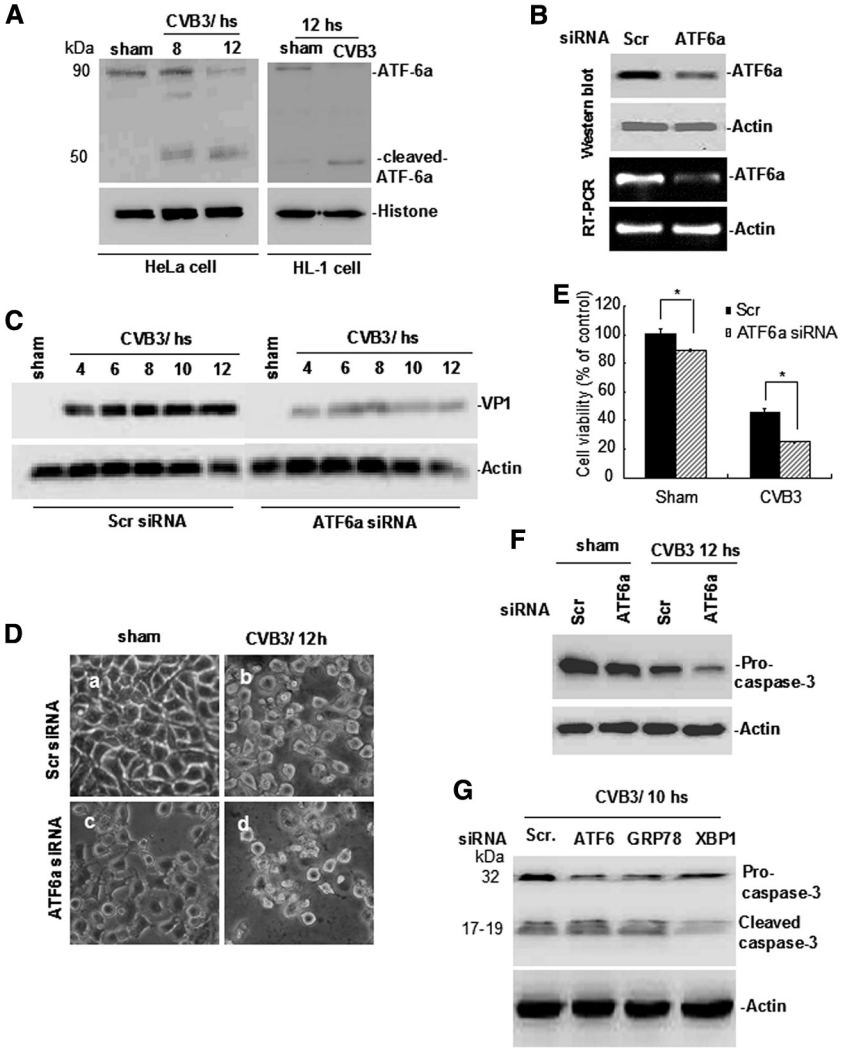

FIG. 5. CVB3 infection induces cleavage of ATF6a, and silencing of ATF6a enhances CVB3-caused cell death and reduces VP1 synthesis. Both HL-1 and HeLa cells were cultured and infected with CVB3 as described for Fig. 1. (A) Cell lysates were prepared and subjected to Western blotting to determine the pattern of ATF6a cleavage. Histone detection serves as a loading control. (B) HeLa cells were transfected with ATF6a siRNA or scrambled siRNA (control). The expression of ATF6a was detected by Western blotting and RT-PCR, as indicated. (C) HeLa cells were infected with CVB3 after siRNA transfection. Cell lysates collected at the indicated time points pi were used to detect VP1 production. (D) Cell morphology was observed by phase-contrast microscopy, and (E) cell viability was measured by MTS assay. The data are presented as a percentage of the control (as described for Fig. 1D). Error bars represent means ± SD. $P < 0.05$. (F) Western blot of cell lysates collected at 12 h pi, detecting procaspase-3 cleavage. (G) The cleavage of caspase-3 was further confirmed on high-percentage gels on which 80 μg of total protein was loaded. Actin detection serves as a loading control.

ensure that the overexpressed HA-ATF6a protein was functional, we performed Western blot analysis to detect the activated form of ATF6a and found that the p50 cleavage product was present in Dox-induced/CVB3-infected cells but not in the three controls, including noninduced/CVB3-infected cells, noninduced/sham-infected cells, and Dox-induced/sham-infected cells, that were incubated for 10 h (Fig. 6A). Since AFT6a is an ER membrane protein, we wanted to rule out the possibility that the activation of the UPR was nonspecifically generated by the overexpression of an ER membrane protein in our experimental system. We therefore detected GRP78 expression levels in HeLa cells transfected with a plasmid pcDNA3.1-ATF6(171-373) overexpressing a dominant-negative (DN) ATF6a and found that the overexpression of DN-ATF6a decreased GRP78 production compared to that of the controls (Fig. 6B). These data indicate that the overexpressed HA-ATF6a is functional and can specifically induce UPR. With the Tet-On/HA-ATF6a cell line, we first evaluated whether ATF6a overexpression could induce the activation of ER chaperones in the absence of CVB3 infection. As shown in Fig. 6C, ATF6a expression was dramatically increased by 12 h pdi. The increased expression of ATF6a, like the increased expression of XBP1 shown in Fig. 2 and 4, induced an overall upregulation of ER chaperone GRP78, although a transient downregulation at 24 to 48 h pdi was observed. The increased ATF6a expression also apparently induced the downregulation of $p58^{IPK}$ and increased the phosphorylation of eIF2α. As expected, the overexpression of ATF6a also upregulated XBP1

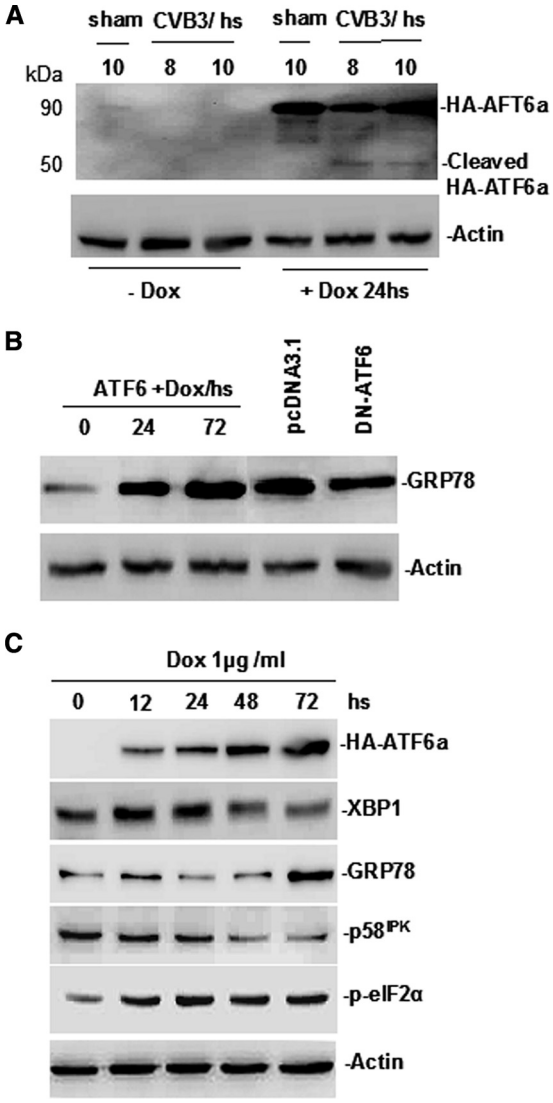

FIG. 6. Overexpression of ATF6a alters target gene expression in the absence of CVB3 infection. (A) CVB3-induced cleavage of HA-ATF6a. Tet-On/HA-ATF6a cells were left uninduced or were induced with Dox and then infected with CVB3 or sham infected with PBS. At the indicated time points pi, the functional form of ATF6a (p50) was detected by Western blot analysis. Actin expression was used as a loading control. (B) The specific induction of the UPR in Dox-induced Tet-On/HA-ATF6a cells. HeLa cells were transfected with either the plasmid pcDNA3.1-ATF6(171-373), which overexpresses a dominant-negative (DN) ATF6a, or with the pcDNA3.1 vector only (as a control), and GRP78 expression was detected by Western blot analysis at 48 h posttransfection. GRP78 detected in Tet-On/ATF6a cells after Dox induction was included as an additional control. (C) Overexpression of ATF6a upregulates XBP1 and alters UPR-responsive gene expression in the absence of CVB3 infection. Tet-On/HA-ATF6a cells were induced or not induced for ATF6a expression. Cell lysates were subjected to Western blot analysis to detect the expression levels of ATF6a and other UPR-related genes using the indicated antibodies.

by 12 h pdi, further confirming that XBP1 is inducible by ATF6a. These data support previous reports that ATF6a can induce XBP1 expression, and that the IRE1 and ATF6a pathways interact with each other and functionally intersect at XBP1 (31, 63). Note that XBP1 protein levels declined at 48 h pdi, which may be due, as reported for XBP1u (64), to a negative regulation targeting the XBP1 protein for proteasome-mediated degradation.

ATF6a overexpression benefits CVB3 replication. CVB3 infection induces ATF6a activation (i.e., cleavage) and initiates the UPR. The UPR affects cell fate by either inducing adaptation to ER stress or by inducing apoptosis (29). CVB3 infection is known to be persistent in the heart (2, 25), implying the sustained activation of ATF6a in cardiomyocytes. To semiquantitatively evaluate the effect of ATF6a expression levels on cell survival and CVB3 replication efficiency, we compared uninduced and induced Tet-On/HA-ATF6a cells at various time points after infection with CVB3. We then evaluated the effect of ATF6a overexpression on (i) CVB3 replication by the Western blot analysis of VP1, (ii) infectious viral particle formation by plaque assay, and (iii) cell viability by MTS assay. The expression of GRP78 and CVB3 VP1 was significantly enhanced from 6 to 10 h pi in cells induced for ATF6a overexpression compared to that of uninduced cells at corresponding time points (Fig. 7A). Enhanced CVB3 VP1 production at 12 h pi was further confirmed by viral plaque assay (Fig. 7B). Finally, Fig. 7C shows that during CVB3 infection, the induction of ATF6a decreased cell viability.

CVB3-induced suppression of $p58^{IPK}$ correlates with upregulation of PKR and phosphorylation of eIF2α. Since the CVB3-activated IRE1-XBP1 pathway and the overexpression of ATF6a was associated with the downregulation of $p58^{IPK}$, a negative regulator of eIF2α kinases PKR and PERK, we next examined if CVB3 infection also could activate PERK or PKR and increase the phosphorylation of eIF2α. HeLa cells were infected with CVB3, and total proteins were analyzed by Western blotting. As shown in Fig. 8A, $p58^{IPK}$ was downregulated, and by 6 h pi the phosphorylation of PKR (p-PKR) had increased. However, we failed to detect an increase in the phosphorylation of PERK (data not shown). Phosphorylated eIF2α (p-eIF2α) production was upregulated at each time point pi.

Overexpression of $p58^{IPK}$ benefits CVB3 replication. $p58^{IPK}$ is a cochaperone in the ER stress response (43). Its upregulation enhances cell survival and, in turn, allows increased viral replication (16). To explore this circuitry, we used the pcDNA1/Neo-$p58^{IPK}$ plasmid to establish a stable HeLa cell line, and we prepared lysates from cells at different time points pi. The level of $p58^{IPK}$ expression and its effect on the phosphorylation of PKR and eIF2α and on the production of CVB3 VP1 protein were evaluated by Western blot analysis. In addition, the resulting viral titers were measured by plaque assay. Figure 8B shows that $p58^{IPK}$ overexpression counteracted the CVB3-induced downregulation of $p58^{IPK}$ and produced an overall net increase in $p58^{IPK}$ production, decreased the phosphorylation of PKR and eIF2α, and increased the synthesis of CVB3 VP1 protein compared to that of a control line of stable cells made by vector-only transfection. Enhanced CVB3 replication was further confirmed by the increased viral titer in the $p58^{IPK}$ stable cells (Fig. 8C).

CVB3 infection induces upregulation of proapoptotic CHOP and activation of SREBP1, caspase-7, and caspase-12. To analyze the ER stress-mediated signal transduction pathway leading to cell apoptosis, we evaluated downstream proapoptotic gene expression in HeLa and HL-1 cells after CVB3 infection. In HeLa cells, CHOP was upregulated, and another ER-asso-

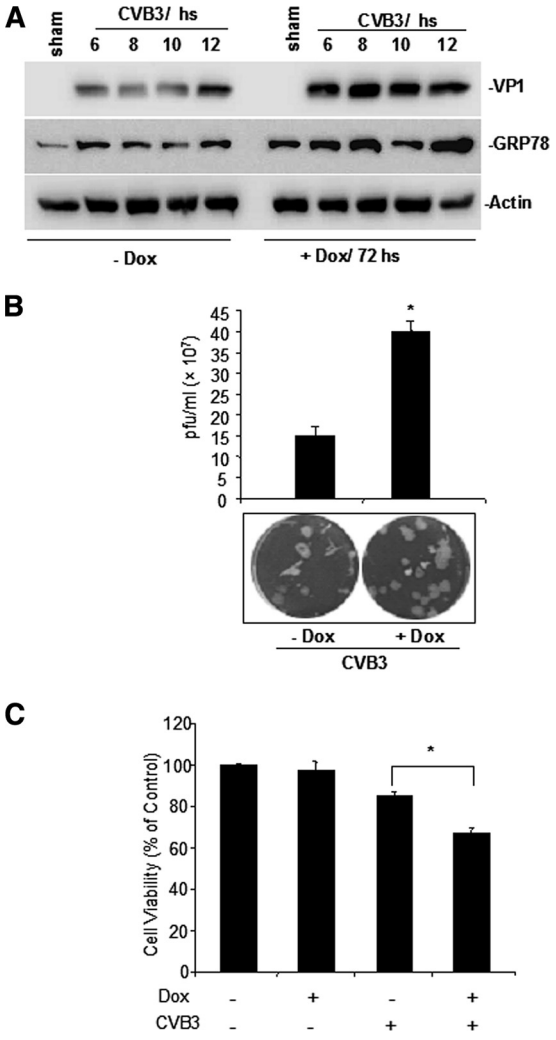

FIG. 7. ATF6a overexpression benefits CVB3 replication. (A) Tet-On/HA-ATF6a HeLa cells were induced or not induced for ATF6a expression and then infected with CVB3. At the indicated time points pi, cell lysates were prepared for Western blot analysis of CVB3 VP1 and GRP78. Actin was detected in parallel as a loading control. (B) Viral plaque assay. The CVB3 titer was determined by plaque assay at 12 h pi. A sample of uninduced cells is included as a control. (C) Cell viability assay. HeLa cells were left uninduced or were induced and then infected with CVB3. Cell viability was determined by MTS assay at 12 h pi. The data are presented as percentages of the uninduced, uninfected control. Error bars represent means ± SD. $P < 0.05$.

ciated transcription factor, SREBP1, an ER stress marker and proapoptotic protein (15), was activated (Fig. 9A). Full-length SREBP1 (125 kDa) was cleaved to produce an ~60-kDa activated product as early as 4 h pi. We also observed some bands with molecular sizes greater than 60 kDa, which likely are nonspecific products, as they did not show an increase in intensity over time, as the SREBP1 cleavage product did. Finally, we detected activated caspase-12, a key marker of ER stress-mediated apoptosis (36), in CVB3-infected HL-1 cells (Fig. 9B). It was not possible to investigate caspase-12 activation in HeLa cells, as no human orthologue of mouse caspase-12 has been clearly identified (14). The activation of caspase-12 in HL-1 cells was further indicated by the activation of caspase-7, an upstream activator of caspase-12 (41) (Fig. 9B). Activated caspase-7 also was apparent in infected HeLa cells (Fig. 9C). The intensity of cleaved caspase-7 product was reduced by 10 h pi in HL-1 cells, perhaps because of proteasome-mediated degradation.

DISCUSSION

CVB3 is a nonenveloped RNA virus, which replicates rapidly in double-layered membrane vesicles derived from the intracellular membrane system (58). Thus, it is not surprising that we found evidence that CVB3 infection induces ER stress response measures. In this study, we explored CVB3-induced ER stress responses and their effects on the induction of apoptosis in an attempt to better understand the molecular pathogenesis of CVB3. We directly examined CVB3-infected cardiomyocytes and HeLa cells and employed inducible HeLa cell lines engineered to overexpress the stress response gene XBP1 or ATF6a. Overall, we found that CVB3 infection induces ER stress and differentially regulates the three arms of the UPR. Specifically, we observed the upregulation of GRP78, the master regulator of the UPR, soon after the CVB3 infection of both HeLa cells and cardiomyocytes. Further, the siRNA silencing of GRP78 enhanced CVB3-induced cell death, indicating that the activation of the UPR early during CVB3 infection promotes host cell survival. Following the upregulation of GRP78 in CVB3-infected cells, the IRE1-mediated splicing of XBP1u was activated and produced XBP1s. As in previous reports (28, 30), XBP1s in turn induced the upregulation of various genes encoding protein degradation and folding factors, including EDEM1 and ERdj4. $p58^{IPK}$ is a negative regulator of PKR and PERK (43, 54) and has been reported to be present at unchanged or heightened levels in cells during infection by various viruses, including influenza virus (43), flaviviruses (66), and mouse hepatitis virus (MHV) (3). Surprisingly, we observed $p58^{IPK}$ to be downregulated at both the mRNA and protein levels in CVB-infected HeLa and HL-1 cells. Furthermore, the induced overexpression of $p58^{IPK}$ increased CVB3 VP1 protein production, implying that $p58^{IPK}$ serves to promote overall host cell health and thereby viral protein production.

In unperturbed cells, GRP78 is associated with the ER stress sensor ATF6a. Upon perturbation they typically disassociate, with ATF6a then invoking the initiation of UPR activities. We explored ATF6a protein expression in both HeLa and HL-1 cells as well as in a Tet-On HeLa cell line inducibly expressing ATF6a, and we found that CVB3 infection activated ATF6a, producing a 50-kDa cleavage product in all three cell types. In the inducible HeLa cells, we found that the increased expression of ATF6a was associated with an overall increase in GRP78 production (Fig. 6C). Further, we observed that ATF6a pathway activation also regulated other components of the UPR. For instance, XBP1, the substrate of IRE1 (63), was upregulated in response to increased ATF6a, in agreement with previous reports suggesting cross-talk between the IRE1-XBP1 and ATF6a pathways of the UPR (31, 63).

$P58^{IPK}$ is an ER luminal cochaperone associated with GRP78 (43). It functions primarily as an inhibitor of the eIF2α protein kinases PERK and PKR (61), thus facilitating translation under normal cellular conditions. Recent evidence shows

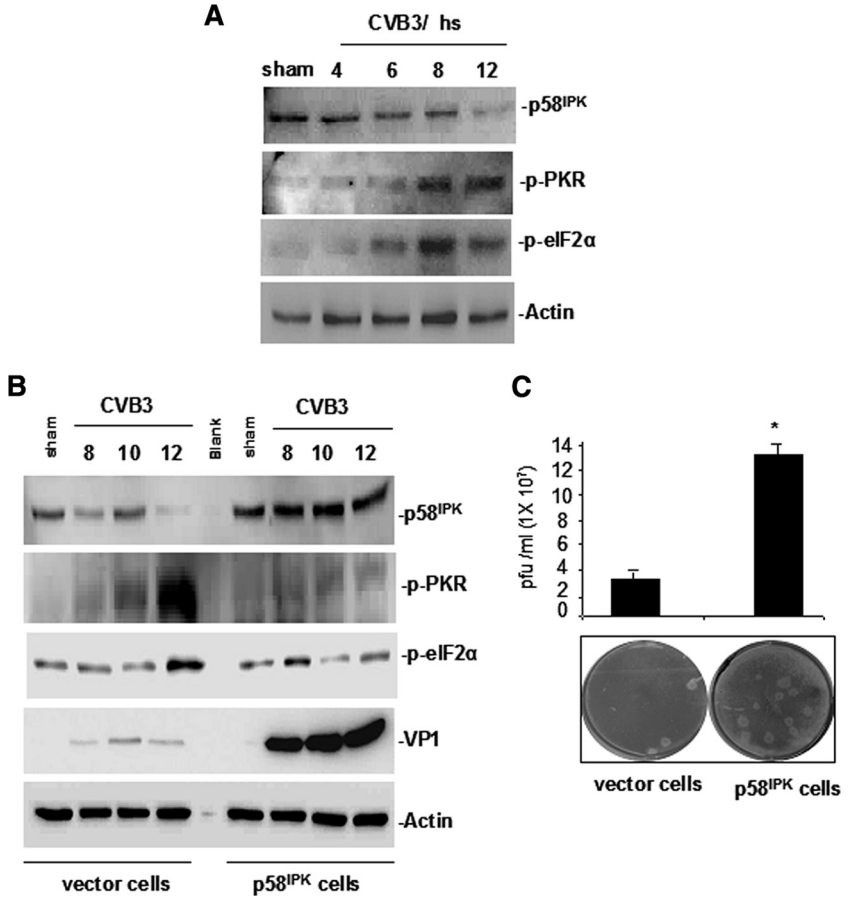

FIG. 8. CVB3-induced downregulation of $p58^{IPK}$ activates PKR-mediated phosphorylation of eIF2α, and overexpression of $p58^{IPK}$ increases CVB3 RNA translation. (A) HeLa cells were cultured and infected with CVB3 as described for Fig. 1. Cell lysates were subjected to Western blot analysis to detect $p58^{IPK}$ and the phosphorylation of PKR and e-IF2α. (B) HeLa cells stably transfected to express $p58^{IPK}$ and vector-transfected cells (as a control) were infected with CVB3 at an MOI of 10. Cell lysates were used to detect $p58^{IPK}$, CVB3 VP1, and phosphorylated PKR and eIF2α at the indicated time point pi. Actin expression is included as a loading control. (C) The results of viral plaque assays measuring viral titers in infected cell samples collected at 12 h pi are shown.

that $p58^{IPK}$ has PERK-independent functions and mediates the cytosolic degradation of misfolded proteins delayed at the ER translocon. Thus, it has been suggested that $p58^{IPK}$ has multiple functions involved in protecting the cell from ER stress (39). Here, $p58^{IPK}$ was downregulated upon ATF6a activation in CVB3-infected HeLa cells and in noninfected, Dox-induced Tet-On/HA-ATF6a cells, further suggesting that $p58^{IPK}$ is involved in cross-talk among the UPR pathways. Our data support the notion that the IRE1-XBP1 pathway is regulated by ATF6a and connected to the PKR (PERK) pathway via $p58^{IPK}$. We note that our data showing the downregulation of $p58^{IPK}$ are inconsistent with a previous report that utilized uninfected, tunicamycin-treated cell cultures (54). The downregulation of $p58^{IPK}$ that we observed in the Tet-On cell line may be related to the specific cellular conditions in these cells, where the induced expression of ATF6a produced the overexpression of XBP1u. It has been reported that XBP1u can form a complex with, and thereby negatively regulate, the UPR-specific transcription factors ATF6a and XBP1s. Once formed, the complex can be sequestered from the nucleus and degraded by proteasomes (64, 65). Thus, the negatively regulated ATF6a and XBP1s in the Tet-On cells may result in the downregulation of $p58^{IPK}$. For this reason, the Tet-On cell system, although useful, may not be as meaningful an experimental system as nontransfected cells for analyzing the effect of ATF6a or XBP1 on CVB3 replication.

We speculate that the lowered expression of $p58^{IPK}$ that we observed during CVB3 infection facilitates persistent PKR signaling, thereby sustaining the enhanced phosphorylation of eIF2α. We note also that p-PERK was not significantly upregulated during CVB3 infection (data not shown), and we assume that p-PERK's role in increasing the phosphorylation of eIF2α during CVB3 infection is compensated for by upregulated p-PKR. It is known that eIF2α phosphorylation can inhibit the translation of eukaryotic cellular mRNAs. However, during CVB3 infection, we observed enhanced VP1 protein production under conditions of increased eIF2α phosphorylation present in cells overexpressing XBP1 or ATF6a. We speculate that robust CVB3 translation under conditions in which host translation is inhibited is enabled by the CVB3 internal ribosome entry site (IRES), which mediates translation initiation in a cap-independent manner (62) and can bypass the eIF2a-dependent translation block (46, 49). In addition, the reduction in the cap-dependent translation of cellular mRNAs

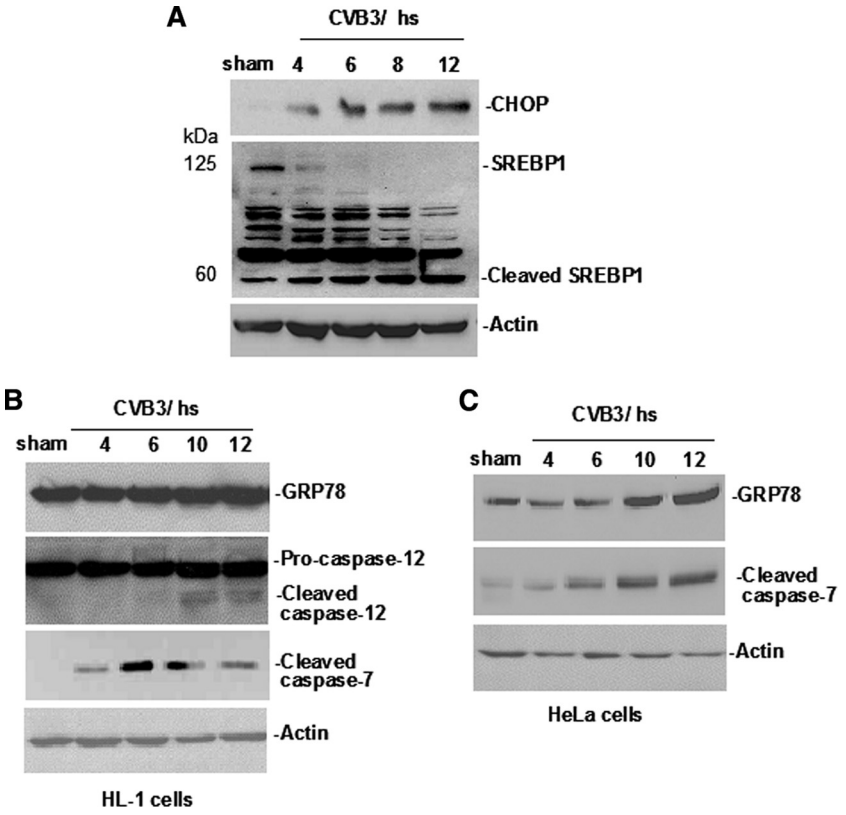

FIG. 9. CVB3 infection induces upregulation of CHOP and activation of SREBP1, caspase-7, and caspase-12. HeLa cells or HL-1 cells were cultured and infected with CVB3 as described in Fig. 1. Cell lysates were subjected to Western blot analysis to detect the induction and activation (cleavage) of proapoptotic transcription factors CHOP and SREBP1, respectively (A), cleavage pattern (indicating activation) of caspases-7 and caspase-12 in HL-1 cells (B), and caspase-7 in HeLa cells (C). Actin was detected in parallel as a loading control.

that occurs during CVB3 infection likely results in the greater availability of translation machinery for the IRES-driven translation of viral RNA (13). It has been reported that HCV, another IRES-containing RNA virus, suppresses cellular XBP1 *trans*-activating activity, leading to the elevated translation of its own mRNA (51). Here, in CVB3-infected cells overexpressing $p58^{IPK}$, the phosphorylation of eIF2a by PKR was downregulated (Fig. 8B), allowing increased cellular mRNA translation and thereby enhanced cellular health and an environment more conducive to CVB3 replication.

In several other experimental systems, the phosphorylation of eIF2α has been associated with an upregulation of ATF4 and the subsequent induction of the proapoptotic transcription factor CHOP (19, 37). We were unable to detect the increased expression of ATF4 during CVB3 infection (data not shown), but we did observe a significant upregulation in the level of CHOP. Since ATF4 and ATF6a work in concert to activate CHOP expression (60), we speculate that the CHOP upregulation we observed during CVB3 infection is modulated primarily by ATF6a.

SREBP1 is another transcription factor associated with the ER membrane. Its function in the regulation of lipid homeostasis has been studied extensively. It was reported that in response to a low level of sterol and other unidentified factors, SREBP1 translocates from the ER to the Golgi complex, where it is cleaved by site-1 and site-2 proteases. The fully processed mature form of SREBP1 then enters the nucleus and transactivates target gene expression (6). The activation of SREBPs by cleavage also was reported to occur in HCV-infected Huh cells (57). In addition, two recent studies reported that SREBP1c activation plays a major role in β-cell glucolipotoxicity and apoptosis (55) and that an increased level of active SREBPs in macrophages is involved in HIV protease inhibitor-induced apoptosis via the depletion of ER calcium stores and the activation of caspase-12 (69). We found that during CVB3 infection SREBP1 was induced, and the level of its cleaved form increased coincidently with the upregulation of p-eIF2α and CHOP as well as with the activation of caspase-7 and -12. A recent report indicated that caspase-7 expression is positively controlled by SREBP1 and SREBP2 (15), thus providing a prospective linkage between SREBP1 and caspase-7 in the apoptosis cascade.

Caspase-12 is an ER membrane-associated cysteine protease that is induced and activated by caspase-7 in response to ER stress (36, 41). It has been suggested that caspase-12 is a key mediator of ER stress-induced apoptosis and is required for the recruitment of other cytosolic caspases to the ER membrane during the induction of the apoptotic program (41). Our results show that caspase-12 was cleavage activated in HL-1 cells by 6 h postinfection, and that this event temporally coincided with the induction of other apoptotic mediators, such as CHOP and caspase-3 and -7, two caspases involved in the

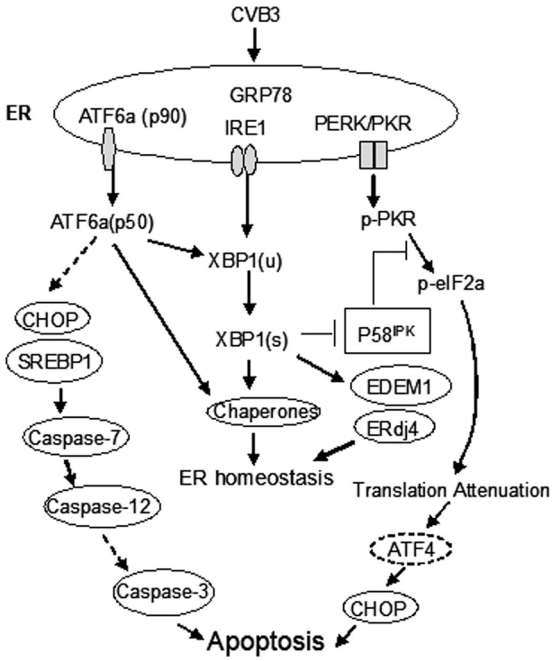

FIG. 10. Proposed model of CVB3-induced ER stress response. CVB3 infection activates three arms of UPR pathways and induces apoptosis through the suppression of $p58^{IPK}$ and the activation of CHOP and SREBP1. Notably, the activation of the proapoptotic transcription factors CHOP and SREBP1 likely is through ATF6a and not ATF4. Dotted lines with arrows indicate tentative relationships requiring further confirmation.

cascade of caspase-12-mediated apoptosis (34). We note that although the human genome contains no identified orthologue of mouse casapse-12 (14), it has two similar speculative counterparts, namely, caspase-4 and caspase-5. A recent study reported that caspase-4 is involved in ER stress (21), but as yet there is no related report on caspase-5. The question of whether caspase-4 and/or caspase-5 plays a role in humans equivalent to that of mouse caspase-12 in mediating apoptosis induction requires further study.

In summary, our studies using both HeLa cells and cardiomyocytes indicate that during CVB3 infection, UPR pathways are induced but are carried out in a manner involving the atypical expression of several UPR target genes, including $p58^{IPK}$, EDEM1, and ERdj4 (Fig. 10). Further, CVB3-induced alterations of UPR pathways can result in the activation of proapoptotic genes, engendering a shift from ER stress pathways to those of apoptosis. Since cardiomyocyte apoptosis is a hallmark of viral myocarditis, these data provide further insight into the molecular pathogenesis of CVB3-induced myocarditis.

ACKNOWLEDGMENTS

We thank Yi-Ling Lin, Michael Katze, and Kazutoshi Mori for providing us the plasmids pHA-XBP1u-GFP, pcDNA1/neo-$p58^{IPK}$, and pcDNA3.1-AFT6(171-373), respectively, and our colleagues Alhousseynou Sall and Kasinath Viswanathan for helpful discussions.

This work was supported by grants from the Canadian Institutes of Health Research and the Heart and Stroke Foundation of BC and Yukon. J.Y. is a recipient of the Doctoral Research Award from the Canadian Institutes of Health Research and Michael Smith Foundation of Health; X.Y. is a recipient of the UGF Award of the University of British Columbia; Z.L. is a recipient of the Doctoral Research Award from the Heart and Stroke Foundation of Canada.

REFERENCES

1. **Abbate, A., G. Sinagra, R. Bussani, N. N. Hoke, M. Merlo, A. Varma, S. Toldo, F. N. Salloum, G. G. Biondi-Zoccai, G. W. Vetrovec, F. Crea, F. Silvestri, and A. Baldi.** 2009. Apoptosis in patients with acute myocarditis. Am. J. Cardiol. **104:**995–1000.
2. **Andréoletti, L., D. Hober, P. Becquart, S. Belaich, M. C. Copin, V. Lambert, and P. Wattre.** 1997. Experimental CVB3-induced chronic myocarditis in two murine strains: evidence of interrelationships between virus replication and myocardial damage in persistent cardiac infection. J. Med. Virol. **52:** 206–214.
3. **Bechill, J., Z. Chen, J. W. Brewer, and S. C. Baker.** 2008. Coronavirus infection modulates the unfolded protein response and mediates sustained translational repression. J. Virol. **82:**4492–4501.
4. **Benali-Furet, N. L., M. Chami, L. Houel, F. De Giorgi, F. Vernejoul, D. Lagorce, L. Buscail, R. Bartenschlager, F. Ichas, R. Rizzuto, and P. Paterlini-Brechot.** 2005. Hepatitis C virus core triggers apoptosis in liver cells by inducing ER stress and ER calcium depletion. Oncogene **24:**4921–4933.
5. **Boyce, M., and J. Yuan.** 2006. Cellular response to endoplasmic reticulum stress: a matter of life or death. Cell Death Differ. **13:**363–373.
6. **Brown, M. S., and J. L. Goldstein.** 1997. The SREBP pathway: regulation of cholesterol metabolism by proteolysis of a membrane-bound transcription factor. Cell **89:**331–340.
7. **Calfon, M., H. Zeng, F. Urano, J. H. Till, S. R. Hubbard, H. P. Harding, S. G. Clark, and D. Ron.** 2002. IRE1 couples endoplasmic reticulum load to secretory capacity by processing the XBP-1 mRNA. Nature **415:**92–96.
8. **Chan, S. W., and P. A. Egan.** 2005. Hepatitis C virus envelope proteins regulate CHOP via induction of the unfolded protein response. FASEB J. **19:**1510–1512.
9. **Chau, D. H., J. Yuan, H. Zhang, P. Cheung, T. Lim, Z. Liu, A. Sall, and D. Yang.** 2007. Coxsackievirus B3 proteases 2A and 3C induce apoptotic cell death through mitochondrial injury and cleavage of eIF4GI but not DAP5/p97/NAT1. Apoptosis **12:**513–524.
10. **Chow, L. H., K. W. Beisel, and B. M. McManus.** 1992. Enteroviral infection of mice with severe combined immunodeficiency. Evidence for direct viral pathogenesis of myocardial injury. Lab. Investig. **66:**24–31.
11. **Claycomb, W. C., N. A. Lanson, Jr., B. S. Stallworth, D. B. Egeland, J. B. Delcarpio, A. Bahinski, and N. J. Izzo, Jr.** 1998. HL-1 cells: a cardiac muscle cell line that contracts and retains phenotypic characteristics of the adult cardiomyocyte. Proc. Natl. Acad. Sci. U. S. A. **95:**2979–2984.
12. **D'Ambrosio, A., G. Patti, A. Manzoli, G. Sinagra, A. Di Lenarda, F. Silvestri, and G. Di Sciascio.** 2001. The fate of acute myocarditis between spontaneous improvement and evolution to dilated cardiomyopathy: a review. Heart **85:** 499–504.
13. **Ehrenfeld, E.** 1984. Picornavirus inhibition of host cell protein synthesis, p. 177–221. *In* H. Fraenkel-Conrat and R. R. Wagner (ed.), Comprehensive virology, vol. 19. Plenum, New York, NY.
14. **Fischer, H., U. Koenig, L. Eckhart, and E. Tschachler.** 2002. Human caspase 12 has acquired deleterious mutations. Biochem. Biophys. Res. Commun. **293:**722–726.
15. **Gibot, L., J. Follet, J. P. Metges, P. Auvray, B. Simon, L. Corcos, and C. Le Jossic-Corcos.** 2009. Human caspase 7 is positively controlled by SREBP-1 and SREBP-2. Biochem. J. **420:**473–483.
16. **Goodman, A. G., J. A. Smith, S. Balachandran, O. Perwitasari, S. C. Proll, M. J. Thomas, M. J. Korth, G. N. Barber, L. A. Schiff, and M. G. Katze.** 2007. The cellular protein P58IPK regulates influenza virus mRNA translation and replication through a PKR-mediated mechanism. J. Virol. **81:**2221–2230.
17. **Grist, N. R., and D. Reid.** 1993. Epidemiology of viral infections of the heart, p. 23–30. *In* J. E. Banatvala (ed.), Viral infection of the heart. Edward Arnold, London, United Kingdom.
18. **Harding, H. P., M. Calfon, F. Urano, I. Novoa, and D. Ron.** 2002. Transcriptional and translational control in the mammalian unfolded protein response. Annu. Rev. Cell Dev. Biol. **18:**575–599.
19. **Harding, H. P., Y. Zhang, A. Bertolotti, H. Zeng, and D. Ron.** 2000. Perk is essential for translational regulation and cell survival during the unfolded protein response. Mol. Cell **5:**897–904.
20. **Haze, K., H. Yoshida, H. Yanagi, T. Yura, and K. Mori.** 1999. Mammalian transcription factor ATF6 is synthesized as a transmembrane protein and activated by proteolysis in response to endoplasmic reticulum stress. Mol. Biol. Cell **10:**3787–3799.
21. **Hitomi, J., T. Katayama, Y. Eguchi, T. Kudo, M. Taniguchi, Y. Koyama, T. Manabe, S. Yamagishi, Y. Bando, K. Imaizumi, Y. Tsujimoto, and M. Tohyama.** 2004. Involvement of caspase-4 in endoplasmic reticulum stress-induced apoptosis and Abeta-induced cell death. J. Cell Biol. **165:**347–356.
22. **Hu, P., Z. Han, A. D. Couvillon, R. J. Kaufman, and J. H. Exton.** 2006. Autocrine tumor necrosis factor alpha links endoplasmic reticulum stress to the membrane death receptor pathway through IRE1alpha-mediated NF-kappaB activation and down-regulation of TRAF2 expression. Mol. Cell. Biol. **26:**3071–3084.
23. **Isler, J. A., A. H. Skalet, and J. C. Alwine.** 2005. Human cytomegalovirus

infection activates and regulates the unfolded protein response. J. Virol. **79:**6890–6899.
24. **Jordan, R., L. Wang, T. M. Graczyk, T. M. Block, and P. R. Romano.** 2002. Replication of a cytopathic strain of bovine viral diarrhea virus activates PERK and induces endoplasmic reticulum stress-mediated apoptosis of MDBK cells. J. Virol. **76:**9588–9599.
25. **Kandolf, R., K. Klingel, R. Zell, H. C. Selinka, U. Raab, W. Schneider-Brachert, and B. Bultmann.** 1993. Molecular pathogenesis of enterovirus-induced myocarditis: virus persistence and chronic inflammation. Intervirology **35:**140–151.
26. **Kaufman, R. J.** 1999. Stress signaling from the lumen of the endoplasmic reticulum: coordination of gene transcriptional and translational controls. Genes Dev. **13:**1211–1233.
27. **Kozutsumi, Y., M. Segal, K. Normington, M. J. Gething, and J. Sambrook.** 1988. The presence of malfolded proteins in the endoplasmic reticulum signals the induction of glucose-regulated proteins. Nature **332:**462–464.
28. **Kurisu, J., A. Honma, H. Miyajima, S. Kondo, M. Okumura, and K. Imaizumi.** 2003. MDG1/ERdj4, an ER-resident DnaJ family member, suppresses cell death induced by ER stress. Genes Cells **8:**189–202.
29. **Larner, S. F., R. L. Hayes, and K. K. Wang.** 2006. Unfolded protein response after neurotrauma. J. Neurotrauma **23:**807–829.
30. **Lee, A. H., N. N. Iwakoshi, and L. H. Glimcher.** 2003. XBP-1 regulates a subset of endoplasmic reticulum resident chaperone genes in the unfolded protein response. Mol. Cell. Biol. **23:**7448–7459.
31. **Lee, K., W. Tirasophon, X. Shen, M. Michalak, R. Prywes, T. Okada, H. Yoshida, K. Mori, and R. J. Kaufman.** 2002. IRE1-mediated unconventional mRNA splicing and S2P-mediated ATF6 cleavage merge to regulate XBP1 in signaling the unfolded protein response. Genes Dev. **16:**452–466.
32. **Liu, Z., H. M. Zhang, J. Yuan, T. Lim, A. Sall, G. A. Taylor, and D. Yang.** 2008. Focal adhesion kinase mediates the interferon-gamma-inducible GTPase-induced phosphatidylinositol 3-kinase/Akt survival pathway and further initiates a positive feedback loop of NF-kappaB activation. Cell Microbiol. **10:**1787–1800.
33. **Luo, H., J. Zhang, F. Dastvan, B. Yanagawa, M. A. Reidy, H. M. Zhang, D. Yang, J. E. Wilson, and B. M. McManus.** 2003. Ubiquitin-dependent proteolysis of cyclin D1 is associated with coxsackievirus-induced cell growth arrest. J. Virol. **77:**1–9.
34. **Masud, A., A. Mohapatra, S. A. Lakhani, A. Ferrandino, R. Hakem, and R. A. Flavell.** 2007. Endoplasmic reticulum stress-induced death of mouse embryonic fibroblasts requires the intrinsic pathway of apoptosis. J. Biol. Chem. **282:**14132–14139.
35. **McManus, B. M., L. H. Chow, J. E. Wilson, D. R. Anderson, J. M. Gulizia, C. J. Gauntt, K. E. Klingel, K. W. Beisel, and R. Kandolf.** 1993. Direct myocardial injury by enterovirus: a central role in the evolution of murine myocarditis. Clin. Immunol. Immunopathol. **68:**159–169.
36. **Nakagawa, T., H. Zhu, N. Morishima, E. Li, J. Xu, B. A. Yankner, and J. Yuan.** 2000. Caspase-12 mediates endoplasmic-reticulum-specific apoptosis and cytotoxicity by amyloid-beta. Nature **403:**98–103.
37. **Novoa, I., Y. Zhang, H. Zeng, R. Jungreis, H. P. Harding, and D. Ron.** 2003. Stress-induced gene expression requires programmed recovery from translational repression. EMBO J. **22:**1180–1187.
38. **Oyadomari, S., and M. Mori.** 2004. Roles of CHOP/GADD153 in endoplasmic reticulum stress. Cell Death Differ. **11:**381–389.
39. **Oyadomari, S., C. Yun, E. A. Fisher, N. Kreglinger, G. Kreibich, M. Oyadomari, H. P. Harding, A. G. Goodman, H. Harant, J. L. Garrison, J. Taunton, M. G. Katze, and D. Ron.** 2006. Cotranslocational degradation protects the stressed endoplasmic reticulum from protein overload. Cell **126:**727–739.
40. **Pavio, N., P. R. Romano, T. M. Graczyk, S. M. Feinstone, and D. R. Taylor.** 2003. Protein synthesis and endoplasmic reticulum stress can be modulated by the hepatitis C virus envelope protein E2 through the eukaryotic initiation factor 2alpha kinase PERK. J. Virol. **77:**3578–3585.
41. **Rao, R. V., E. Hermel, S. Castro-Obregon, G. del Rio, L. M. Ellerby, H. M. Ellerby, and D. E. Bredesen.** 2001. Coupling endoplasmic reticulum stress to the cell death program. Mechanism of caspase activation. J. Biol. Chem. **276:**33869–33874.
42. **Reimold, A. M., A. Etkin, I. Clauss, A. Perkins, D. S. Friend, J. Zhang, H. F. Horton, A. Scott, S. H. Orkin, M. C. Byrne, M. J. Grusby, and L. H. Glimcher.** 2000. An essential role in liver development for transcription factor XBP-1. Genes Dev. **14:**152–157.
43. **Rutkowski, D. T., S. W. Kang, A. G. Goodman, J. L. Garrison, J. Taunton, M. G. Katze, R. J. Kaufman, and R. S. Hegde.** 2007. The role of p58IPK in protecting the stressed endoplasmic reticulum. Mol. Biol. Cell **18:**3681–3691.
44. **Rutkowski, D. T., and R. J. Kaufman.** 2004. A trip to the ER: coping with stress. Trends Cell Biol. **14:**20–28.
45. **Saraste, A., A. Arola, T. Vuorinen, V. Kyto, M. Kallajoki, K. Pulkki, L. M. Voipio-Pulkki, and T. Hyypia.** 2003. Cardiomyocyte apoptosis in experimental coxsackievirus B3 myocarditis. Cardiovasc. Pathol. **12:**255–262.
46. **Schröder, M., and R. J. Kaufman.** 2005. The mammalian unfolded protein response. Annu. Rev. Biochem. **74:**739–789.
47. **Shen, J., X. Chen, L. Hendershot, and R. Prywes.** 2002. ER stress regulation of ATF6 localization by dissociation of BiP/GRP78 binding and unmasking of Golgi localization signals. Dev. Cell **3:**99–111.
48. **Si, X., H. Luo, A. Morgan, J. Zhang, J. Wong, J. Yuan, M. Esfandiarei, G. Gao, C. Cheung, and B. M. McManus.** 2005. Stress-activated protein kinases are involved in coxsackievirus B3 viral progeny release. J. Virol. **79:**13875–13881.
49. **Szegezdi, E., S. E. Logue, A. M. Gorman, and A. Samali.** 2006. Mediators of endoplasmic reticulum stress-induced apoptosis. EMBO Rep. **7:**880–885.
50. **Tan, M., J. R. Gallegos, Q. Gu, Y. Huang, J. Li, Y. Jin, H. Lu, and Y. Sun.** 2006. SAG/ROC-SCF beta-TrCP E3 ubiquitin ligase promotes pro-caspase-3 degradation as a mechanism of apoptosis protection. Neoplasia **8:**1042–1054.
51. **Tardif, K. D., K. Mori, R. J. Kaufman, and A. Siddiqui.** 2004. Hepatitis C virus suppresses the IRE1-XBP1 pathway of the unfolded protein response. J. Biol. Chem. **279:**17158–17164.
52. **Tirasophon, W., A. A. Welihinda, and R. J. Kaufman.** 1998. A stress response pathway from the endoplasmic reticulum to the nucleus requires a novel bifunctional protein kinase/endoribonuclease (Ire1p) in mammalian cells. Genes Dev. **12:**1812–1824.
53. **Tirosh, B., N. N. Iwakoshi, B. N. Lilley, A. H. Lee, L. H. Glimcher, and H. L. Ploegh.** 2005. Human cytomegalovirus protein US11 provokes an unfolded protein response that may facilitate the degradation of class I major histocompatibility complex products. J. Virol. **79:**2768–2779.
54. **van Huizen, R., J. L. Martindale, M. Gorospe, and N. J. Holbrook.** 2003. P58IPK, a novel endoplasmic reticulum stress-inducible protein and potential negative regulator of eIF2alpha signaling. J. Biol. Chem. **278:**15558–15564.
55. **Wang, H., G. Kouri, and C. B. Wollheim.** 2005. ER stress and SREBP-1 activation are implicated in beta-cell glucolipotoxicity. J. Cell Sci. **118:**3905–3915.
56. **Wang, X. Z., H. P. Harding, Y. Zhang, E. M. Jolicoeur, M. Kuroda, and D. Ron.** 1998. Cloning of mammalian Ire1 reveals diversity in the ER stress responses. EMBO J. **17:**5708–5717.
57. **Waris, G., D. J. Felmlee, F. Negro, and A. Siddiqui.** 2007. Hepatitis C virus induces proteolytic cleavage of sterol regulatory element binding proteins and stimulates their phosphorylation via oxidative stress. J. Virol. **81:**8122–8130.
58. **Wong, J., J. Zhang, X. Si, G. Gao, I. Mao, B. M. McManus, and H. Luo.** 2008. Autophagosome supports coxsackievirus B3 replication in host cells. J. Virol. **82:**9143–9153.
59. **Wu, J., and R. J. Kaufman.** 2006. From acute ER stress to physiological roles of the unfolded protein response. Cell Death Differ. **13:**374–384.
60. **Wu, J., D. T. Rutkowski, M. Dubois, J. Swathirajan, T. Saunders, J. Wang, B. Song, G. D. Yau, and R. J. Kaufman.** 2007. ATF6alpha optimizes long-term endoplasmic reticulum function to protect cells from chronic stress. Dev. Cell **13:**351–364.
61. **Yan, W., C. L. Frank, M. J. Korth, B. L. Sopher, I. Novoa, D. Ron, and M. G. Katze.** 2002. Control of PERK eIF2alpha kinase activity by the endoplasmic reticulum stress-induced molecular chaperone P58IPK. Proc. Natl. Acad. Sci. U. S. A. **99:**15920–15925.
62. **Yang, D., J. E. Wilson, D. R. Anderson, L. Bohunek, C. Cordeiro, R. Kandolf, and B. M. McManus.** 1997. In vitro mutational and inhibitory analysis of the cis-acting translational elements within the 5′ untranslated region of coxsackievirus B3: potential targets for antiviral action of antisense oligomers. Virology **228:**63–73.
63. **Yoshida, H., T. Matsui, A. Yamamoto, T. Okada, and K. Mori.** 2001. XBP1 mRNA is induced by ATF6 and spliced by IRE1 in response to ER stress to produce a highly active transcription factor. Cell **107:**881–891.
64. **Yoshida, H., M. Oku, M. Suzuki, and K. Mori.** 2006. pXBP1(U) encoded in XBP1 pre-mRNA negatively regulates unfolded protein response activator pXBP1(S) in mammalian ER stress response. J. Cell Biol. **172:**565–575.
65. **Yoshida, H., A. Uemura, and K. Mori.** 2009. pXBP1(U), a negative regulator of the unfolded protein response activator pXBP1(S), targets ATF6 but not ATF4 in proteasome-mediated degradation. Cell Struct. Funct. **34:**1–10.
66. **Yu, C. Y., Y. W. Hsu, C. L. Liao, and Y. L. Lin.** 2006. Flavivirus infection activates the XBP1 pathway of the unfolded protein response to cope with endoplasmic reticulum stress. J. Virol. **80:**11868–11880.
67. **Yuan, J., P. K. Cheung, H. M. Zhang, D. Chau, and D. Yang.** 2005. Inhibition of coxsackievirus B3 replication by small interfering RNAs requires perfect sequence match in the central region of the viral positive strand. J. Virol. **79:**2151–2159.
68. **Yuan, J., D. A. Stein, T. Lim, D. Qiu, S. Coughlin, Z. Liu, Y. Wang, R. Blouch, H. M. Moulton, P. L. Iversen, and D. Yang.** 2006. Inhibition of coxsackievirus B3 in cell cultures and in mice by peptide-conjugated morpholino oligomers targeting the internal ribosome entry site. J. Virol. **80:**11510–11519.
69. **Zhou, H., W. M. Pandak, Jr., V. Lyall, R. Natarajan, and P. B. Hylemon.** 2005. HIV protease inhibitors activate the unfolded protein response in macrophages: implication for atherosclerosis and cardiovascular disease. Mol. Pharmacol. **68:**690–700.